NEURAL REGENERATION RESEARCH
October 2014, Volume 9, Issue 19
www.nrronline.org

Adenosine monophosphate-activated protein kinase activation enhances embryonic neural stem cell apoptosis in a mouse model of amyotrophic lateral sclerosis

Yanling Sui, Zichun Zhao, Rong Liu, Bin Cai, Dongsheng Fan

Department of Neurology, Peking University Third Hospital, Beijing, China

Corresponding author:
Dongsheng Fan, M.D., Ph.D., Department of Neurology, Peking University Third Hospital, 49 North Garden Road, Haidian District, Beijing 100191, China, wshns99@163.com.

doi:*10.4103/1673-5374.143421*
http:*//www.nrronline.org/*

Accepted: *2014-07-22*

Abstract

Alterations in embryonic neural stem cells play crucial roles in the pathogenesis of amyotrophic lateral sclerosis. We hypothesized that embryonic neural stem cells from $SOD1^{G93A}$ individuals might be more susceptible to oxidative injury, resulting in a propensity for neurodegeneration at later stages. In this study, embryonic neural stem cells obtained from human superoxide dismutase 1 mutant ($SOD1^{G93A}$) and wild-type ($SOD1^{WT}$) mouse models were exposed to H_2O_2. We assayed cell viability with mitochondrial succinic dehydrogenase colorimetric reagent, and measured cell apoptosis by flow cytometry. Moreover, we evaluated the expression of the adenosine monophosphate-activated protein kinase (AMPK) α-subunit, paired box 3 (Pax3) protein, and p53 in western blot analyses. Compared with $SOD1^{WT}$ cells, $SOD1^{G93A}$ embryonic neural stem cells were more likely to undergo H_2O_2-induced apoptosis. Phosphorylation of AMPKα in $SOD1^{G93A}$ cells was higher than that in $SOD1^{WT}$ cells. Pax3 expression was inversely correlated with the phosphorylation levels of AMPKα. p53 protein levels were also correlated with AMPKα phosphorylation levels. Compound C, an inhibitor of AMPKα, attenuated the effects of H_2O_2. These results suggest that embryonic neural stem cells from $SOD1^{G93A}$ mice are more susceptible to apoptosis in the presence of oxidative stress compared with those from wild-type controls, and the effects are mainly mediated by Pax3 and p53 in the AMPKα pathway.

Key Words: *nerve regeneration; neuroderegeneration; embryonic neural stem cells; adenosine monophosphate-activated protein kinase α; paired box 3; p53; $SOD1^{G93A}$ mouse; amyotrophic lateral sclerosis; oxidative stress; hydrogen peroxide; apoptosis; NSFC grants; neural regeneration*

Funding: *This work was supported by a grant from the National Natural Sciences Foundation of China, No. 81030019.*

Sui YL, Zhao ZC, Liu R, Cai B, Fan DS. Adenosine monophosphate-activated protein kinase activation enhances embryonic neural stem cell apoptosis in a mouse model of amyotrophic lateral sclerosis. Neural Regen Res. 2014;9(19):1770-1778.

Introduction

Amyotrophic lateral sclerosis is a fatal neurodegenerative disease. To date, many related genes and loci have been identified in this disease (Beleza-Meireles and Al-Chalabi, 2009; Maruyama et al., 2010; DeJesus-Hernandez et al., 2011). Mutations in superoxide dismutase 1 (SOD1) account for 20% of cases of familial amyotrophic lateral sclerosis and 5% of sporadic cases (Rosen, 1993). Several mutations of human SOD1 ($SOD1^{G93A}$, $SOD1^{G37R}$, and $SOD1^{G85R}$) have been investigated in a mouse model (Gurney et al., 1994; Bruijn et al., 1997; Cai and Fan, 2013; Ye et al., 2013). Of these mutant forms, $SOD1^{G93A}$ is the most common. Initial studies detected no significant pathology during the early course of the disease (Gurney et al., 1994). However, several recent reports have shown that pathological and physiological changes occur much earlier than previously thought, even at the embryonic stage. Embryonic alterations in motor neuronal morphology induce hyperexcitability in adult-onset $SOD1^{G93A}$ mice (Martin et al., 2013). Studies on neonatal neuronal circuitry have also shown a hyperexcitable disturbance in $SOD1^{G93A}$ mice (van Zundert et al., 2008). Progressive degeneration of lumbar motor neurons in $SOD1^{G93A}$ transgenic mice has also been suggested to occur at birth (Lowry et al., 2001). In addition to mature neural cells, Luo et al. (2007) recently reported an impairment of SDF1/CXCR4 signaling, which regulates neural development *via* the promotion of cell survival and proliferation, in neural stem cells (NSCs) derived from $SOD1^{G93A}$ mice. Abnormalities in embryonic NSCs might result in susceptibility to neurodegeneration at a later stage. Thus, identification of early alterations in NSCs might be crucial to understand amyotrophic lateral sclerosis pathogenesis.

Adenosine monophosphate-activated protein kinase (AMPK) is a central regulator of cellular metabolism. It consists of a catalytic α-subunit and regulatory β- and γ-subunits (Ma et al, 2012). The Thr172 residue of the α-subunit is phosphorylated under specific conditions such as exercise, hypoxia, and oxidative stress (Hardie, 2007). However, the full array of AMPK functions has not yet been elucidated in NSCs, although there have been studies on other neural cell types. For example, AMPK protects embryonic hippocampal neurons

from hypoxia-induced cell death and partially guards against oxidative stress-induced cell death in an immortalized cerebellar cell line (Culmsee et al., 2001; Park et al., 2009). Nuclear translocation of AMPK potentiates striatal neurodegeneration (Ju et al., 2011). Furthermore, AMPK regulates forkhead box, class O, mammalian target of rapamycin, and mammalian silent information regulator 2 ortholog (Fulco et al., 2003; Cheng et al., 2004; Greer et al., 2007; Canto et al., 2009), which have been implicated in NSC regulation. Recently, Loken et al. (2012) suggested that AMPK mediates the effects of oxidative stress on neural tube development. It remains to be determined whether AMPK exhibits protective or cell death-inducing effects on NSCs under conditions of oxidative stress.

The aim of the present study was to investigate the effects of hydrogen peroxide (H_2O_2)-induced oxidative stress on embryonic NSCs in the $SOD1^{G93A}$ mouse model of amyotrophic lateral sclerosis and evaluate whether AMPK has certain effects on NSCs under conditions of oxidative stress.

Materials and Methods

Isolation and culture of NSCs

Fetal mice used in this study were bred under the strain designations B6SJL-Tg($SOD1^{G93A}$)1Gur/J and B6SJL-Tg (SOD1)2Gur/J for $SOD1^{G93A}$ transgenic and wild-type SOD1 transgenic mice. They were obtained from Jackson Laboratories (Gurney et al., 1994). Brains were removed from the embryos at embryonic day 14 to isolate NSCs, as described previously (Park et al., 2012), with slight modifications. Animal care and experimental protocols were performed in strict accordance with *the NIH Guide for the Care and Use of Laboratory Animals* and were approved by the Animal Care and Ethics Committee at Peking University Third Hospital, China.

Each embryo was genotyped by genomic polymerase chain reaction (PCR) using primers for the hSOD1 transgene (forward: 5′-CAT CAG CCC TAA TCC ATC TGA-3′; reverse: 5′-CGC GAC TAA CAA TCA AAG TGA-3′). NSCs prepared from $SOD1^{G93A}$ fetal mice (carrying the human $SOD1^{G93A}$ gene) and $SOD1^{WT}$ fetal mice (carrying the human wild-type SOD1 gene) were used for experiments. $SOD1^{WT}$ NSCs served as controls. After the meninges were removed, single cell suspensions were obtained by mechanical dissociation. Then, the cell suspensions were centrifuged at 100 × *g* for 5 minutes. After discarding the supernatant, the cells were re-suspended with 1 mL complete neurosphere medium. The cells were seeded at a density of 2×10^5/mL in 10 mL complete NSC medium. NSCs were cultured in maintenance medium containing Dulbecco's modified Eagle medium/Ham's F-12 medium (DMEM/F12) supplemented with serum-free neurobasal growth supplement 2% v/v (B27, Life Technologies, Carlsbad, CA, USA), recombinant human basic fibroblast growth factor (20 ng/mL, PeproTech, Rocky Hill, NJ, USA), and recombinant human epidermal growth factor (20 ng/mL, PeproTech) in a humidified incubator (37°C, 5% CO_2). Neurospheres with diameters of about 200 μm were sub-cultured after 3–5 days.

Test groups

After genotyping, $SOD1^{G93A}$ NSCs and $SOD1^{WT}$ NSCs were exposed to 0.5 mmol/L H_2O_2, 1 mmol/L H_2O_2, or normal conditions. To elucidate the role of AMPK in H_2O_2-induced apoptosis of NSCs, we employed an AMPK activator (5-aminoimidazole-4-carboxyamide ribonucleoside, AICAR) or inhibitor (compound C). The NSCs were divided into four groups: normal, H_2O_2, AICAR (positive control), and H_2O_2 plus compound C. The 3% (w/w) H_2O_2 solution, AICAR, and compound C were obtained from Sigma-Aldrich (St Louis, MO, USA).

Immunocytochemistry

NSCs (4×10^5/mL) were cultured on coverslips coated with poly-L-ornithine (Sigma-Aldrich) for 36 hours. The cells were then incubated with the following primary antibodies at 4°C overnight for double immunolabeling: mouse anti-Nestin monoclonal antibody (1:100; Abcam, Cambridge, MA, USA) and rabbit anti-Sox2 monoclonal antibody (1:100; Epitomics, Burlingame, CA, USA). Then, the cells were incubated with anti-rabbit IgG (1:100) and anti-mouse IgG (1:100) secondary antibodies conjugated with Alexa Fluor® 488 or 594 (Invitrogen, Carlsbad, CA, USA) at room temperature for 1 hour. Lastly, the cells were mounted in mounting medium containing 4′,6-diamidino-2-phenylindole (DAPI; Vector Laboratories, Burlingame, CA, USA). Fluorescence images were captured using an upright fluorescence microscope (Leica, Wetzlar, Hesse-Darmstadt, Germany). Controls for negative staining were prepared with PBS in place of the primary antibodies.

Cell viability and proliferation assays

NSCs were seeded onto poly-L-ornithine-coated 96-well plates at a density of 1×10^4/mL for 36 hours, and then cultured under the four conditions listed above. Then, the culture medium was removed and replaced with normal medium. A total of 10 μL mitochondrial succinic dehydrogenase colorimetric reagent (Cell Counting Kit-8 reagent, Dojindo Laboratories, Kumamoto, Japan) was added to each well according to the manufacturer's protocol, followed by incubation for 3 hours at 37°C with 5% CO_2. The absorbance was measured at 450 nm on a microplate reader (Bio-Rad Laboratories, Hercules, CA, USA) at a reference wavelength of 600 nm.

Flow cytometric analysis

Fluorescein isothiocyanate and propidium iodide (FITC Annexin V Apoptosis Detection Kit, BD Biosciences, Franklin Lakes, NJ, USA) were used to assess NSC apoptosis. Intact cells were Annexin V(–)/PI(–). Early and late apoptotic cells were Annexin V(+)/PI(–) and Annexin V(+)/PI(+), respectively. Necrotic cells were Annexin V(–)/PI(+).

Western blot analysis

NSCs were lysed in RIPA lysis buffer (Apply Technologies, Beijing, China) in the presence of protease and phosphatase inhibitors (Sigma-Aldrich) on ice according to the manufacturer's instructions. The protein concentration was measured with a BCA™ Protein Assay Kit (Pierce Chemical, Rockford, IL, USA). Samples containing 30 μg protein were separated by SDS-polyacrylamide gel electrophoresis and transferred

Table 1 Primer sequence and product size of real-time PCR analyses

Gene	Primer sequence	Product size (bp)
AMPKα1	Forward: 5′-GTA AAC CCC TAT TAT TTG CGT G-3′	222
	Reverse: 5′-TTC GGC ATC AGA GTC ACT CC-3′	
AMPKα2	Forward: 5′-GCT AAG GAC TGA CTC TTA ATT GG-3′	136
	Reverse: 5′-AAC GGC TTC TCA CAC ACA TCT-3′	
Pax3	Forward: 5′-GCA TGG ATT TTC AAG CTA TAC AG-3′	248
	Reverse: 5′-GCA GAC TGT CCA CAT TCT TCA T-3′	
p53	Forward: 5′-CTT CAG TTC ATT GGG ACC ATC-3′	298
	Reverse: 5′-TCC ATA AGC CTG AAA ATG TCT C-3′	
β-Actin	Forward: 5′-CCT AGC ACC ATG AAG ATC AAG AT-3′	130
	Reverse: 5′-ACT CAT CGT ACT CCT GCT TGC T-3′	

to nitrocellulose filter membranes (Millipore, Billerica, MA, USA). The membranes were incubated at 4°C overnight with the following primary antibodies: rabbit anti-AMPKα (1:1,000), rabbit anti-phospho-AMPKα (1:1,000), mouse anti-p53 (1:1,000; Cell Signaling Technology, Boston, MA, USA), and goat anti-paired box 3 (Pax3, 1:250; Abcam, Cambridge, MA, USA). A mouse anti-β-actin antibody (1:1,000; Earthox, San Francisco, CA, USA) was used to label β-actin for normalization. The gray value of protein bands was detected using an infrared imaging system (Odyssey, LICOR Biosciences, Lincoln, NE, USA).

RNA preparation and real-time PCR

Total RNA from NSCs was isolated using a single-step RNA extraction reagent (Trizol, Life Technologies) according to the manufacturer's instructions. The cDNA was synthesized from 1 μg total RNA using avian myeloblastosis virus reverse transcriptase (Reverse Transcription System, Promega, Madison, WI, USA) and amplified by PCR (GoTaq® qPCR Master Mix, Promega). The PCR conditions were as follows: 95°C for 2 minutes and then 40 cycles of 95°C for 15 seconds and 58°C for 30 seconds. The primer sequences are listed in **Table 1**. The expression level of the target gene was normalized to mouse β-actin, and the relative gene expression ($2^{-\triangle\triangle Ct}$) was calculated using the previous method (Livak and Schmittgen, 2001).

Statistical analysis

Data are presented as the mean ± SD. Statistical analyses were performed with SPSS 19.0 software (SPSS, Chicago, IL, USA) using one-way analysis of variance followed by the least significant difference *post-hoc* test. Differences were considered significant at $P < 0.05$.

Results

Culture and identification of mouse embryonic NSCs

SOD1^{G93A} and SOD1^{WT} NSCs were isolated from fetal brains, expanded as neurospheres, and passaged every 3–5 days (**Figure 1**). There was no substantial difference in the formation of neurospheres between the two types of NSCs. In immunofluorescence analyses, most of the cells were positive for the intermediate filament protein Nestin and the transcription factor Sox2 (**Figure 2**), which are markers of NSCs.

Effect of H_2O_2-induced oxidative stress on the apoptosis of NSCs from SOD1^{G93A} mice

To evaluate differences in the susceptibilities of SOD1^{G93A} and SOD1^{WT} NSCs to oxidative stress, the NSCs were exposed to H_2O_2 (0.5 and 1 mmol/L) for 12 hours. As expected, the viability of the NSCs was significantly decreased by H_2O_2 treatment in a dose-dependent manner (**Figure 3A**, $P = 0.004$, $P = 0.016$). Importantly, the viability of SOD1^{G93A} NSCs was significantly more decreased than that of SOD1^{WT} cells when treated with 1 mmol/L H_2O_2 ($P = 0.026$). To further investigate the effects of H_2O_2 on NSC proliferation, cell viability was examined at several time points (0, 24, 48, and 72 hours). In untreated controls, no significant difference was observed in the proliferation of SOD1^{G93A} and SOD1^{WT} cells (**Figure 3B**). However, when 1 mmol/L H_2O_2 was added at 24 hours, cell proliferation was inhibited to 72 hours, and the viability of SOD1^{G93A} NSCs at 72 hours was significantly lower than that of the SOD1^{WT} NSCs. To evaluate the degree of injury induced by H_2O_2 in NSCs, apoptosis was assessed by Annexin V-FITC and PI staining using flow cytometry (**Figure 4A**). Consistent with the observations in the cell viability assay, apoptosis was significantly enhanced by H_2O_2 treatment. When SOD1^{WT} and SOD1^{G93A} NSCs were not treated with H_2O_2, the percentages of apoptotic cells were 13.31 ± 1.21% and 12.57 ± 1.87%, respectively. When SOD1^{WT} and SOD1^{G93A} NSCs were treated with 0.5 mmol/L H_2O_2, the percentages of apoptotic cells increased from 13.31 ± 1.21% and 12.57 ± 1.87% to 20.52 ± 3.04% and 23.43 ± 2.45% ($P = 0.01$ and $P = 0.002$), respectively. When SOD1^{WT} and SOD1^{G93A} NSCs were treated with 1 mmol/L H_2O_2, the percentage of apoptotic cells increased from 13.31% ± 1.21% and 12.57 ± 1.87% to 26.22 ± 2.47% and 35.06 ± 2.95% ($P = 0.026$ and $P = 0.001$), respectively (**Figure 4B**). In the 1 mmol/L H_2O_2 group, the percentage of apoptotic SOD1^{G93A} NSCs was significantly higher than that of SOD1^{WT} cells ($P = 0.029$). These results suggest that SOD1^{G93A} NSCs are more susceptible to oxidative stress induced by H_2O_2.

AMPK phosphorylation was enhanced in H_2O_2-treated SOD1^{G93A} NSCs together with changes in Pax3 and p53 levels

To address the potential role of AMPK in the apoptosis of SOD1^{G93A} and SOD1^{WT} NSCs, we evaluated phosphorylation of AMPKα (**Figure 5A**). Cells were cultured for 36 hours followed by H_2O_2 treatment. Significant increases in the phosphorylation of AMPKα occurred after 12 hours of H_2O_2 exposure, which was markedly higher in SOD1^{G93A} NSCs than that in SOD1^{WT} cells in the 1 mmol/L H_2O_2 group (**Figure 5B**; $P = 0.019$). AMPK has been also shown to inhibit Pax3 expression in a mouse model of diabetic embryopathy (Wu et al., 2012). To confirm our hypothesis that Pax3 expression is also regulated by AMPK in this model,

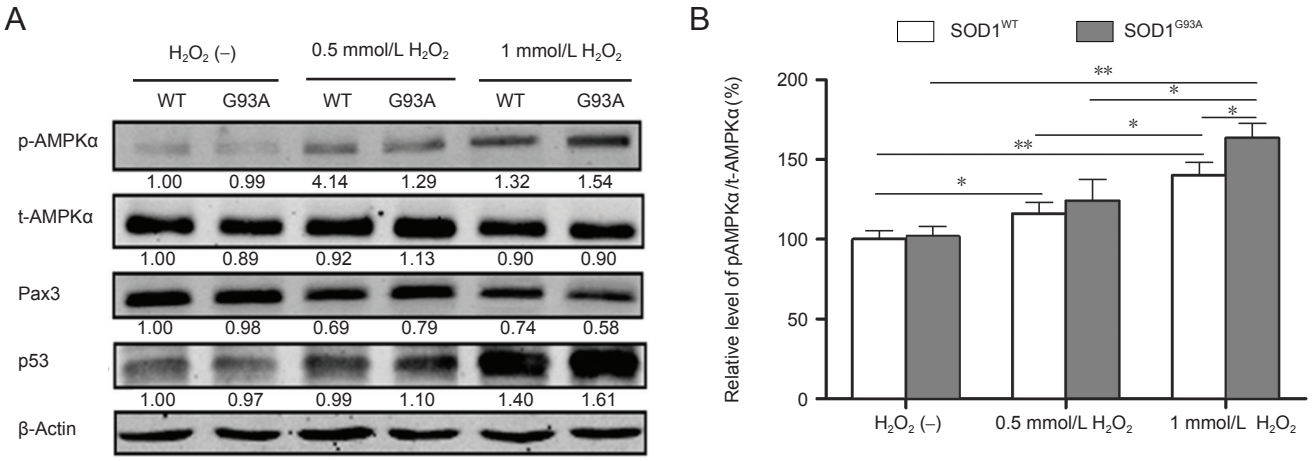

Figure 5 Adenosine monophosphate-activated protein kinase (AMPK) phosphorylation levels are increased in SOD1^{G93A} neural stem cells (NSCs) by H_2O_2 exposure with corresponding changes in Pax3 and p53 levels (western blot analysis).

(A) Representative western blots displaying expression or activation of AMPK α-subunit (AMPKα), paired box 3 (Pax3), and p53 in NSCs treated with or without H_2O_2. β-Actin was used as a loading control. Data below each lane represent the relative gray scale compared with β-actin control bands. Values below SOD1^{WT} NSCs treated without H_2O_2 were set as 1. (B) Phosphorylation levels of AMPKα were quantified relative to the total AMPKα level. The expression level in untreated SOD1^{WT} NSCs was set at 100%. $*P < 0.05$; $**P < 0.01$. Data are presented as the mean ± SD and analyzed using one-way analysis of variance followed by the least significant difference *post-hoc* test. (–): Untreated; WT: superoxide dismutase 1 wild-type neural stem cells; G93A: SOD1^{G93A} neural stem cells; p-AMPKα: phosphorylated AMPKα; t-AMPKα: total AMPKα. SOD1: Superoxide dismutase 1.

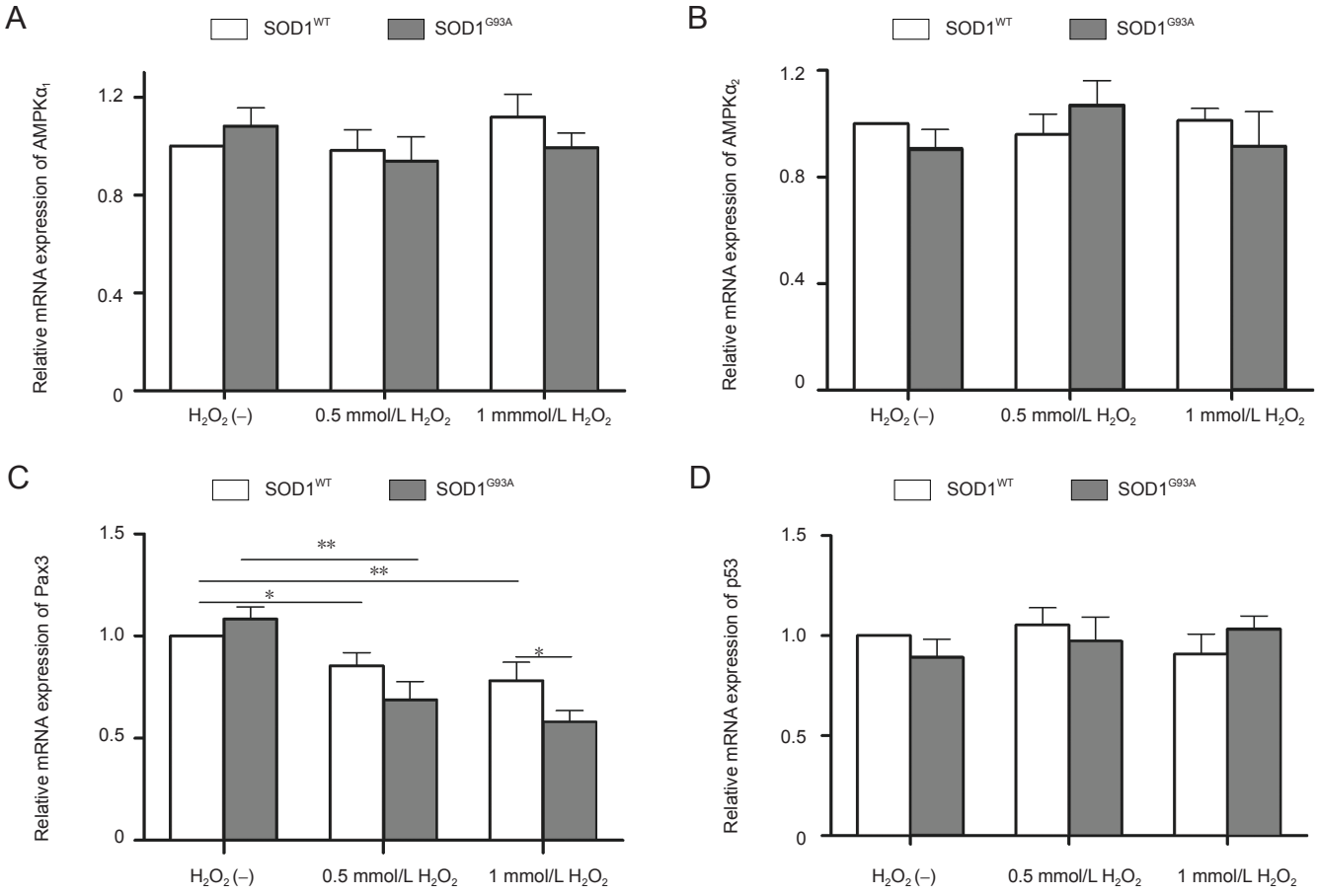

Figure 6 Quantitative real-time PCR analysis of the mRNA expression of adenosine monophosphate (AMP)-activated protein kinase α1 subunit (AMPKα$_1$) (A), AMP-activated protein kinase α2 subunit (AMPKα$_2$) (B), paired box 3 (Pax3) (C), and p53 (D) in neural stem cells under different treatment conditions.

H_2O_2 (–): Untreated. $*P < 0.05$; $**P < 0.01$. Data are presented as the mean ± SD and analyzed using one-way analysis of variance followed by the least significant difference *post-hoc* test. SOD1: Superoxide dismutase 1.

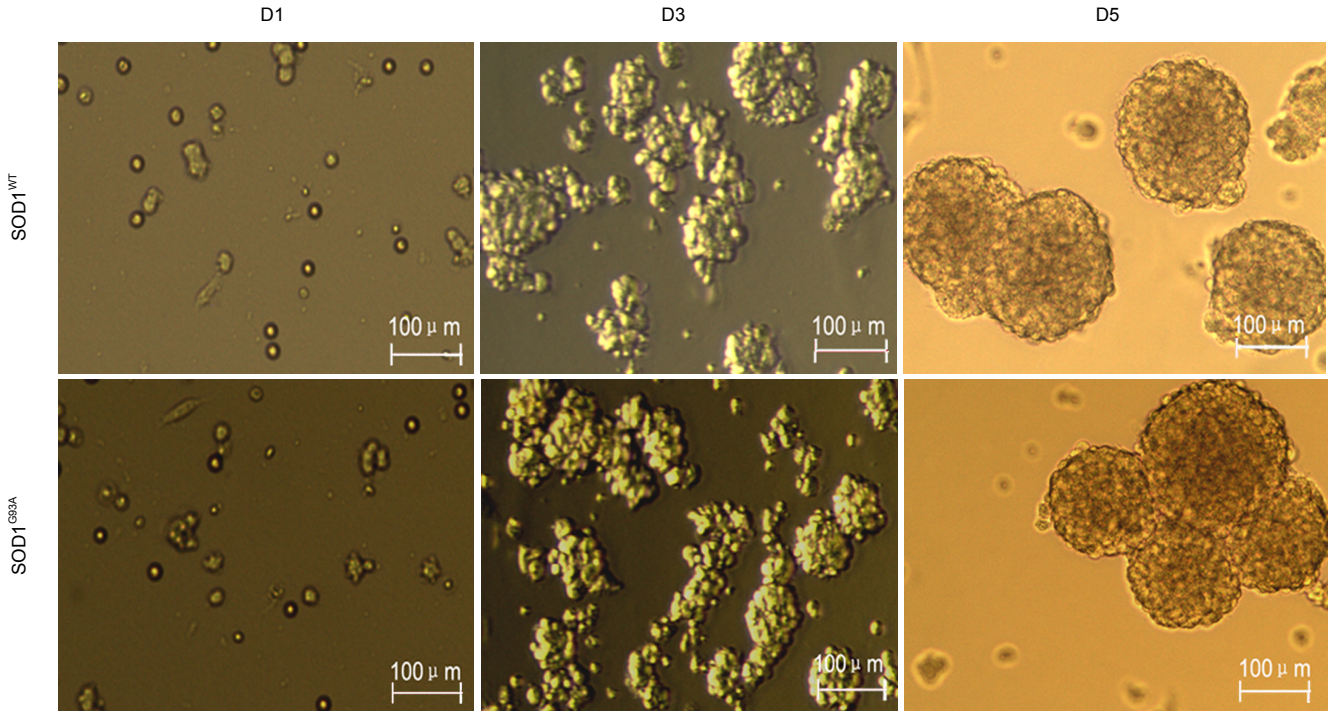

Figure 1 Morphology of neural stem cells prepared from embryos of SOD1^{WT} and SOD1^{G93A} mice at 1, 3, and 5 days after culture (D1, 3, and 5) (inverted microscope).
Embryonic neural stem cells formed typical neurospheres after *in vitro* culture. SOD1: Superoxide dismutase 1.

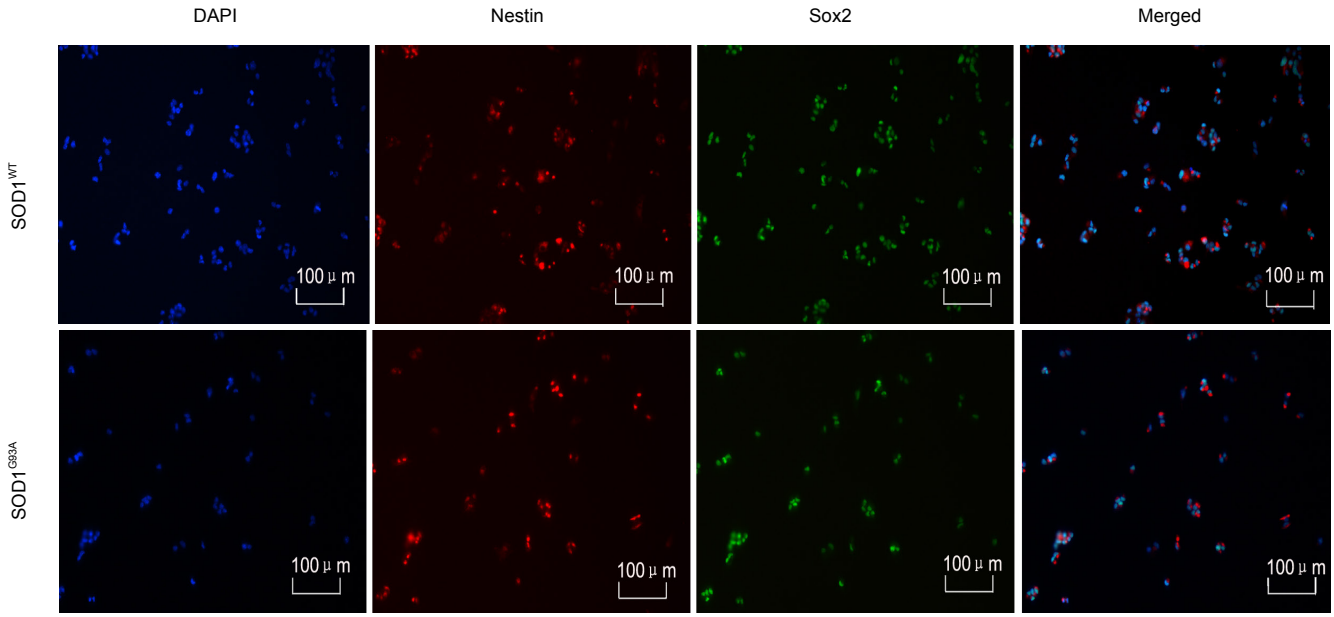

Figure 2 Identification of neural stem cells by double immunofluorescence staining of Nestin (red) and Sox2 (green) (immunocytochemistry, fluorescence microscope).
Nestin and Sox2 were expressed in the neural stem cells derived from mouse embryos. Blue: DAPI-labeled nuclei. SOD1: Superoxide dismutase 1.

we examined Pax3 protein levels (**Figure 5A**). As a result, we found that Pax3 protein levels were clearly decreased in NSCs exposed to H_2O_2, and these changes were more obvious in SOD1^{G93A} NSCs treated with 1 mmol/L H_2O_2. A loss of Pax3 expression has been shown to increase p53 protein levels and apoptosis, resulting in neural tube defects (Chappell et al., 2009). When we examined p53 protein levels (**Figure 5A**), we found an inverse correlation in the concentrations of p53 and Pax3 proteins, *i.e.*, downregulation of Pax3 protein levels enhanced the levels of p53 protein. The above data indicated that the AMPK pathway might be involved in the apoptosis of NSCs induced by H_2O_2.

In addition, we found that the mRNA levels of AMPKα_1, AMPKα_2, and p53 were unaffected by H_2O_2 treatment (**Figure**

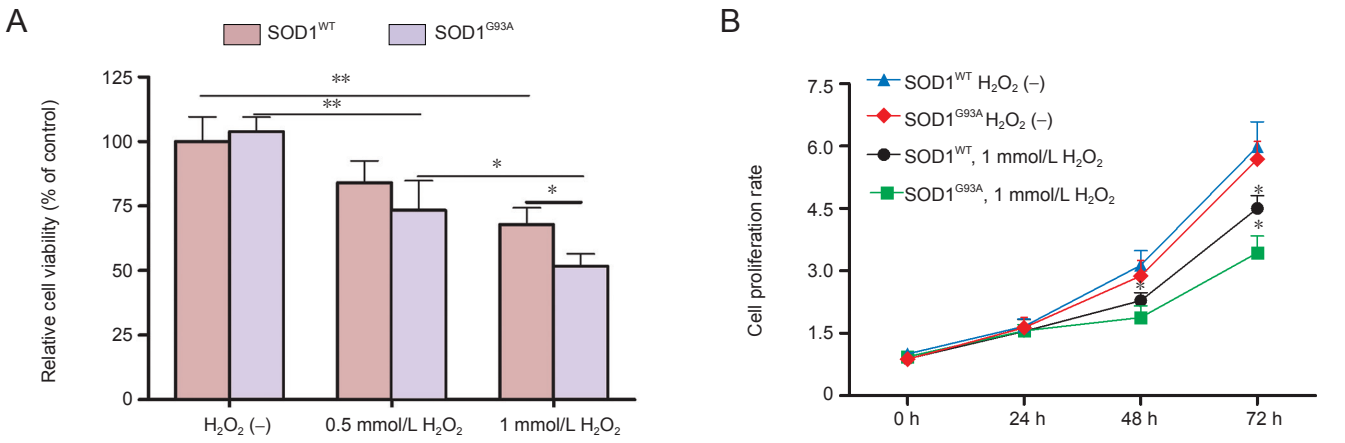

Figure 3 Neural stem cells (NSCs) in SOD1^{G93A} mice are more susceptible to oxidative injury induced by H_2O_2 (cell viability and proliferation assays).
(A) Effects of H_2O_2 on the cell viability of NSCs. The absorbance value of untreated SOD1^{WT} NSCs was set as 100%. (B) Effect of H_2O_2 on the proliferation of NSCs. $*P < 0.05$; $**P < 0.01$. Data are presented as the mean ± SD and analyzed using one-way analysis of variance followed by the least significant difference *post-hoc* test. Each set of measurements was performed in triplicate in at least five independent experiments. H_2O_2 (–) indicates no treatment; h: hour(s); SOD1: superoxied dismutase 1.

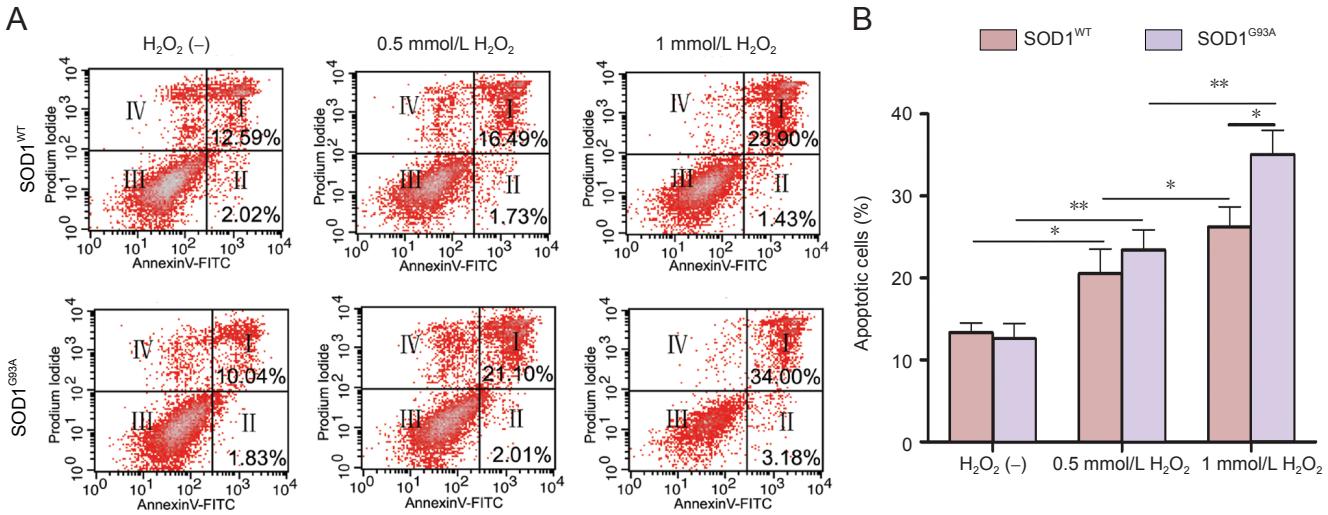

Figure 4 Neural stem cells (NSCs) in SOD1^{G93A} mice are more susceptible to apoptosis induced by H_2O_2 (flow cytometry).
(A) Representative scatter plots showing apoptosis in H_2O_2-treated NSCs by Annexin V-FITC and PI staining and flow cytometry. (I) Late apoptotic cells; (II) early apoptotic cells; (III) intact cells; (IV) necrotic cells. (B) Quantification of apoptotic cells. NSCs were cultured for 36 hours and then treated with H_2O_2 for 12 hours, followed by apoptosis detection. $*P < 0.05$; $**P < 0.01$. The values are the mean ± SD of five independent experiments (one-way analysis of variance followed by the least significant difference *post-hoc* test). H_2O_2 (–) indicates no treatment. SOD1: Superoxide dismutase 1.

6A, B, and **D**). The downregulation of Pax3 mRNA by H_2O_2 treatment was statistically significant, and Pax3 mRNA was significantly lower in SOD1^{G93A} NSCs compared with that in SOD1^{WT} NSCs in the 1 mmol/L H_2O_2 group (**Figure 6C**).

Inhibition of AMPK activity cancelled the effects of H_2O_2 on the apoptosis of NSCs

To further confirm the role of AMPK in H_2O_2-induced apoptosis of NSCs, we employed an AMPK activator (AICAR, 1 mmol/L) and inhibitor (compound C, 1 μmol/L). Cells were maintained in growth medium for 36 hours prior to treatment with different agents. Based on our previous results, 1 mmol/L H_2O_2 was used in these experiments. Compared with controls, NSCs treated with AICAR for 12 hours in the absence of H_2O_2 demonstrated a decrease in viability, although this effect was not significant compared with that in H_2O_2-treated cells (**Figure 7A**; $P = 0.009$ and $P = 0.001$). When NSCs were preincubated for 1 hour with compound C followed by H_2O_2 treatment for 12 hours, cell viability was slightly but significantly reversed compared with that in the 1 mmol/L H_2O_2 group. The cell viability of SOD1^{G93A} NSCs was also similar to SOD1^{WT} cells when treated with 1 mmol/L H_2O_2 plus compound C (**Figure 7A**; $P = 0.431$). Similar results were obtained in cell apoptosis assays (**Figure 7B**). Next, we investigated the effect of AICAR and compound C on the phosphorylation of AMPKα and protein levels of Pax3 and p53 in NSCs using western blot analyses (**Figure 8A**). Similar to H_2O_2 treatment, phosphorylation of AMPKα was increased in response to AICAR. In contrast, compound C inhibited H_2O_2-induced AMPKα phosphorylation. There

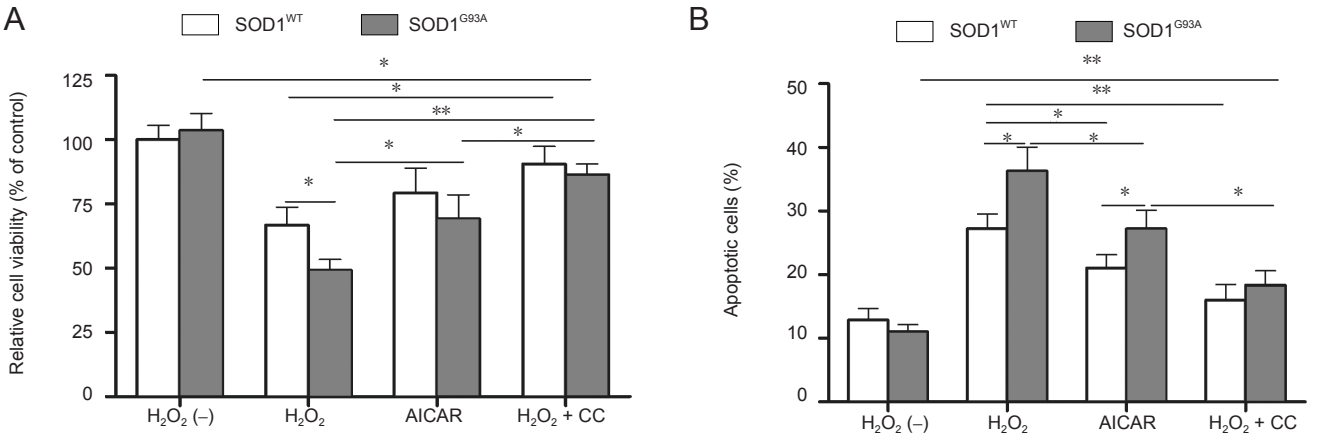

Figure 7 Effects of adenosine monophosphate-activated protein kinase (AMPK) activator 5-aminoimidazole-4-carboxyamide ribonucleoside (AICAR) and inhibitor compound (CC) on the viability and apoptosis of neural stem cells (NSCs).
(A) Cell viability was significantly affected by the addition of AICAR or compound C. The absorbance value of untreated superoxide dismutase 1 wild-type ($SOD1^{WT}$) NSCs was set at 100%. (B) Quantitative assessment of NSC apoptosis by AnnexinV-FITC and PI staining and flow cytometry under different treatment conditions. H_2O_2 (–): Untreated. $*P < 0.05$; $**P < 0.01$. Data are presented as the mean ± SD and analyzed using one-way analysis of variance followed by the least significant difference *post-hoc* test. FITC: Fluoresscen isothiocyante; PI: propidium iodide.

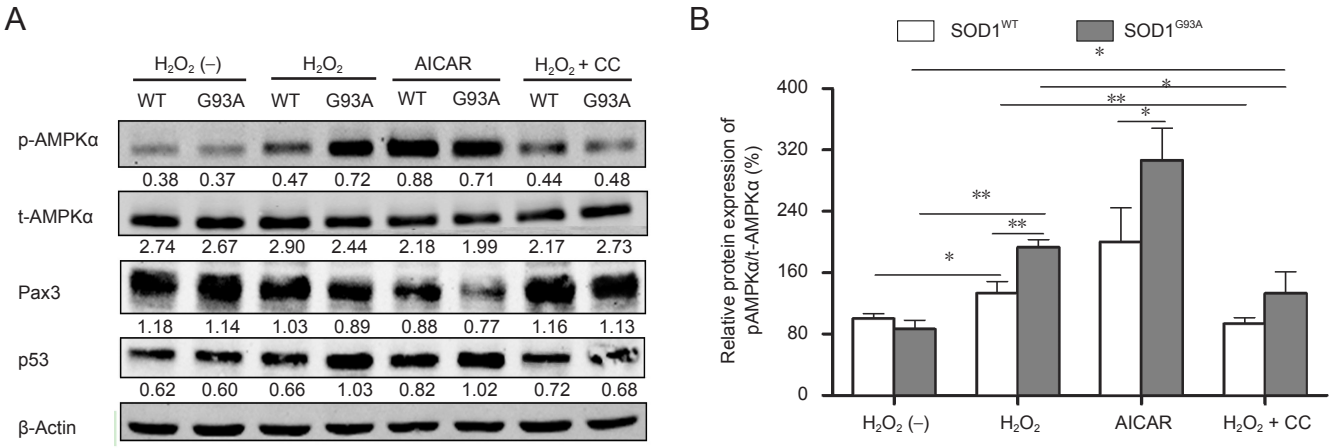

Figure 8 Effects of adenosine monophosphate-activated protein kinase (AMPK) activator 5-aminoimidazole-4-carboxyamide ribonucleoside (AICAR) and inhibitor compound (CC) on the phosphorylation of AMPKα and protein levels of Pax3 and p53 in neural stem cells (NSCs) (western blot analysis).
(A) Representative western blots displaying the phosphorylation of AMPKα, paired box 3 (Pax3), and p53 protein in NSCs exposed to different factors. β-Actin was used as a loading control. Data below each lane represent the relative gray scale compared with β-actin control bands. (B) Phosphorylation levels of AMPKα relative to total AMPKα levels. The expression level in untreated superoxide dismutase 1 wild-type ($SOD1^{WT}$) NSCs was set at 100%. Data are presented as the mean ± SD and analyzed using one-way analysis of variance followed by the least significant difference *post-hoc* test. p-AMPKα: Phosphorylated AMPKα; t-AMPKα: total AMPKα; H_2O_2 (–): Untreated; WT: $SOD1^{WT}$ NSCs; G93A: $SOD1^{G93A}$ NSCs $*P < 0.05$; $**P < 0.01$; SOD1: Superoxide dismutase 1.

was no significant difference in AMPKα phosphorylation of $SOD1^{G93A}$ and $SOD1^{WT}$ NSCs when treated with 1 mmol/L H_2O_2 plus compound C (**Figure 8B**). Pax3 expression was inversely correlated with the changes in AMPKα phosphorylation of H_2O_2- and AICAR-treated NSCs with AICAR treatment producing the most pronounced decrease in Pax3 levels. Pax3 expression was partially restored by compound C in H_2O_2-treated NSCs (**Figure 8A**). Moreover, p53 protein levels were enhanced by AICAR, whereas the effects of H_2O_2 on p53 were partially blocked by compound C. In summary, inhibition of AMPK activity attenuated the effect of H_2O_2 on NSCs. The above data indicate that AMPK activation triggers p53-dependent apoptosis of NSCs induced by H_2O_2.

Discussion

The mechanism underlying mutant SOD1 toxicity has not yet been elucidated. Although some mutants of SOD1 (such as A4V and G85R) exhibit reduced dismutase activity, other mutants (such as G37R and G93A) retain full dismutase activity (Yim et al., 1996). Because $SOD1^{G93A}$ displays full dismutase activity, the mutation itself may not result in apoptosis, which is consistent with the observation that the cell viability of $SOD1^{G93A}$ and $SOD1^{WT}$ NSCs is similar under normal conditions. However, the SOD1 mutation might make cells more vulnerable to oxidative stress. For example, Rogers and Schor (2010) indicated that proteins involved in neurodegenerative disease often play critical roles in early

development of the central nervous system. SOD1 contributes to the organogenesis of embryos, including neurogenesis (Kase et al., 2012). Therefore, it is unclear why the disease appears later in life. Smith proposed a "two-hit" hypothesis for neurodegenerative diseases such as Alzheimer's disease, Parkinson's disease, and amyotrophic lateral sclerosis (Zhu et al., 2004, 2007). The first "hit" is usually a genetic factor, which presents a vulnerability, and the second "hit" is an environmental factor that triggers the neurodegenerative process. This hypothesis is consistent with our observation that, compared with $SOD1^{WT}$ NSCs, more $SOD1^{G93A}$ NSCs were apoptotic when treated with 1 mmol/L H_2O_2. This finding demonstrated that expression of the $SOD1^{G93A}$ gene increased the vulnerability of NSCs to oxidative stress. The "two-hit" hypothesis may also explain why Alzheimer's disease, Parkinson's disease, and amyotrophic lateral sclerosis are age-related diseases. Reactive oxygen species gradually increase with age. When reactive oxygen species increase to a specific threshold, neuronal degeneration may be triggered in some individuals with the mutant gene.

Li et al. (2012) examined rat neural progenitor cells and found that $SOD1^{G93A}$ overexpression increases the cellular sensitivity to oxidative stress. However, elucidation of the pathway underlying $SOD1^{G93A}$ susceptibility has not been studied. In the present study, significant increases in the phosphorylation of AMPKα and relevant changes in Pax3 and p53 levels occurred in the presence of H_2O_2, indicating involvement of the AMPK/Pax3/p53 signaling pathway in the H_2O_2-induced apoptosis of NSCs. Interestingly, phosphorylation of AMPKα and subsequent changes in Pax3 and p53 levels were markedly greater in $SOD1^{G93A}$ NSCs compared with those in $SOD1^{WT}$ cells in the 1 mmol/L H_2O_2 group. These data suggest that activation of the AMPK pathway likely leads to excessive apoptosis of $SOD1^{G93A}$ NSCs. Further experiments using the AMPK activator and inhibitor also clearly indicated that activation of the AMPK/Pax3/p53 pathway mediated the susceptibility of $SOD1^{G93A}$ mutant cells to oxidative stress. However, the AMPK activator and inhibitor had partial effects with regard to H_2O_2 alone, which implies the involment of other cell death signaling pathways such as caspases.

Activated AMPK can also undergo nuclear translocation and regulate gene expression by phosphorylating nuclear proteins (Ju et al., 2011). Based on the data in **Figures 5** and **6**, AMPK inhibited Pax3 transcription, but the underlying mechanism requires further study. In addition, the protein levels of p53 were inversely correlated with those of Pax3, although the mRNA levels of p53 showed no significant change upon downregulation of Pax3 mRNA. These results were consistent with a previous study demonstrating that Pax3 induces p53 ubiquitination and degradation independent of transcription (Wang et al., 2011). Thus, Pax3 is required to block p53-dependent apoptosis and suppression of Pax3 facilitates p53-dependent apoptosis.

Many recent studies have focused on bioenergetic abnormalities in amyotrophic lateral sclerosis. Both amyotrophic lateral sclerosis patients and two commonly used mutant SOD1 mice (G86R and G93A mice) display increased resting energy expenditure, a hypermetabolic phenotype, and compromised mitochondrial function (Dupuis et al., 2004, 2011; Bouteloup et al., 2009; Funalot et al., 2009; Chiang et al., 2010). These metabolic abnormalities have been associated with activation of the energy sensor AMPK. The activity of AMPK is increased in the spinal cords of mutant SOD1 mice, and reducing AMPK activity either pharmacologically or genetically prevents mutant SOD1-induced motor neuron death *in vitro* (Lim et al., 2012). In this study, we investigated the correlation of AMPK with amyotrophic lateral sclerosis. We found that AMPK activation promoted the apoptosis of embryonic NSCs induced by oxidative stress in $SOD1^{G93A}$ mice. In addition to embryonic NSCs, we should draw attention to adult and transplanted NSCs. The pathological processes of motor neuron degeneration stimulats NSC proliferation and neurogenesis in amyotrophic lateral sclerosis patients and adult $SOD1^{G93A}$ mice (Chi et al., 2006; Guan et al., 2007; Galan et al., 2011). Human NSCs are emerging as a promising cellular therapy for amyotrophic lateral sclerosis. Implanted NSCs secrete high levels of the trophic factors that protect spared motor neurons, integrate into the parenchyma, and may differentiate into neurons, astrocytes, and oligodendrocytes (Hefferan et al., 2012; Teng et al., 2012). However, the survival of transplanted NSCs over time is a challenge because of the altered niche in amyotrophic lateral sclerosis (Liu and Martin, 2006). Therefore, it is important to assess whether AMPK regulates adult NSC proliferation and the survival of implanted NSCs.

In conclusion, our data indicate that activation of the AMPK/Pax3/p53 pathway promotes the apoptosis of $SOD1^{G93A}$ NSCs induced by oxidative stress. Thus, AMPK/Pax3/p53 might represent a novel target for protecting $SOD1^{G93A}$ NSCs from oxidative injury, which might also contribute to amyotrophic lateral sclerosis therapy.

Acknowledgments: *We are very grateful to the staff from Clinical Stem Cell Research Center, Peking University Third Hospital, China for their excellent technical assistance.*

Author contributions: *Sui YL, Zhao ZC, Liu R and Cai B contributed to the study design, acquisition and analysis of data, and drafting the article. Fan DS was responsible for the conception and design of the study and revising the article for important intellectual content. All authors approved the final version of the paper.*

Conflicts of interest: *None declared.*

References

Beleza-Meireles A, Al-Chalabi A (2009) Genetic studies of amyotrophic lateral sclerosis: controversies and perspectives. Amyotroph Lateral Scler 10:1-14.

Bouteloup C, Desport JC, Clavelou P, Guy N, Derumeaux-Burel H, Ferrier A, Couratier P (2009) Hypermetabolism in ALS patients: an early and persistent phenomenon. J Neurol 256:1236-1242.

Bruijn LI, Becher MW, Lee MK, Anderson KL, Jenkins NA, Copeland NG, Sisodia SS, Rothstein JD, Borchelt DR, Price DL, Cleveland DW (1997) ALS-linked SOD1 mutant G85R mediates damage to astrocytes and promotes rapidly progressive disease with SOD1-containing inclusions. Neuron 18:327-338.

Cai B, Fan DS (2013) Germline degradation of a mouse model of familial amyotrophic lateral sclerosis when breeding. Zhongguo Zuzhi Gongcheng Yanjiu 17:4521-4528.

Canto C, Gerhart-Hines Z, Feige JN, Lagouge M, Noriega L, Milne JC, Elliott PJ, Puigserver P, Auwerx J (2009) AMPK regulates energy expenditure by modulating NAD+ metabolism and SIRT1 activity. Nature 458:1056-1060.

Chappell JH Jr., Wang XD, Loeken MR (2009) Diabetes and apoptosis: neural crest cells and neural tube. Apoptosis 14:1472-1483.
Cheng SW, Fryer LG, Carling D, Shepherd PR (2004) Thr2446 is a novel mammalian target of rapamycin (mTOR) phosphorylation site regulated by nutrient status. J Biol Chem 279:15719-15722.
Chi L, Ke Y, Luo C, Li B, Gozal D, Kalyanaraman B, Liu R (2006) Motor neuron degeneration promotes neural progenitor cell proliferation, migration, and neurogenesis in the spinal cords of amyotrophic lateral sclerosis mice. Stem Cells 24:34-43.
Chiang PM, Ling J, Jeong YH, Price DL, Aja SM, Wong PC (2010) Deletion of TDP-43 down-regulates Tbc1d1, a gene linked to obesity, and alters body fat metabolism. Proc Natl Acad Sci U S A 107:16320-16324.
Culmsee C, Monnig J, Kemp BE, Mattson MP (2001) AMP-activated protein kinase is highly expressed in neurons in the developing rat brain and promotes neuronal survival following glucose deprivation. J Mol Neurosci 17:45-58.
DeJesus-Hernandez M, Mackenzie IR, Boeve BF, Boxer AL, Baker M, Rutherford NJ, Nicholson AM, Finch NA, Flynn H, Adamson J, Kouri N, Wojtas A, Sengdy P, Hsiung GY, Karydas A, Seeley WW, Josephs KA, Coppola G, Geschwind DH, Wszolek ZK (2011) Expanded GGGGCC hexanucleotide repeat in noncoding region of C9ORF72 causes chromosome 9p-linked FTD and ALS. Neuron 72:245-256.
Dupuis L, Oudart H, Rene F, Gonzalez de Aguilar JL, Loeffler JP (2004) Evidence for defective energy homeostasis in amyotrophic lateral sclerosis: benefit of a high-energy diet in a transgenic mouse model. Proc Natl Acad Sci U S A 101:11159-11164.
Dupuis L, Pradat PF, Ludolph AC, Loeffler JP (2011) Energy metabolism in amyotrophic lateral sclerosis. Lancet Neurol 10:75-82.
Fulco M, Schiltz RL, Iezzi S, King MT, Zhao P, Kashiwaya Y, Hoffman E, Veech RL, Sartorelli V (2003) Sir2 regulates skeletal muscle differentiation as a potential sensor of the redox state. Mol Cell 12:51-62.
Funalot B, Desport JC, Sturtz F, Camu W, Couratier P (2009) High metabolic level in patients with familial amyotrophic lateral sclerosis. Amyotroph Lateral Scler 10:113-117.
Galan L, Gomez-Pinedo U, Vela-Souto A, Guerrero-Sola A, Barcia JA, Gutierrez AR, Martinez-Martinez A, Jimenez MS, Garcia-Verdugo JM, Matias-Guiu J (2011) Subventricular zone in motor neuron disease with frontotemporal dementia. Neurosci Lett 499:9-13.
Greer EL, Oskoui PR, Banko MR, Maniar JM, Gygi MP, Gygi SP, Brunet A (2007) The energy sensor AMP-activated protein kinase directly regulates the mammalian FOXO3 transcription factor. J Biol Chem 282:30107-30119.
Guan YJ, Wang X, Wang HY, Kawagishi K, Ryu H, Huo CF, Shimony EM, Kristal BS, Kuhn HG, Friedlander RM (2007) Increased stem cell proliferation in the spinal cord of adult amyotrophic lateral sclerosis transgenic mice. J Neurochem 102:1125-1138.
Gurney ME, Pu H, Chiu AY, Dal Canto MC, Polchow CY, Alexander DD, Caliendo J, Hentati A, Kwon YW, Deng HX (1994) Motor neuron degeneration in mice that express a human Cu, Zn superoxide dismutase mutation. Science 264:1772-1775.
Hardie DG (2007) AMP-activated/SNF1 protein kinases: conserved guardians of cellular energy. Nat Rev Mol Cell Biol 8:774-785.
Hefferan MP, Galik J, Kakinohana O, Sekerkova G, Santucci C, Marsala S, Navarro R, Hruska-Plochan M, Johe K, Feldman E, Cleveland DW, Marsala M (2012) Human neural stem cell replacement therapy for amyotrophic lateral sclerosis by spinal transplantation. PLoS One 7:e42614.
Ju TC, Chen HM, Lin JT, Chang CP, Chang WC, Kang JJ, Sun CP, Tao MH, Tu PH, Chang C, Dickson DW, Chern Y (2011) Nuclear translocation of AMPK-alpha1 potentiates striatal neurodegeneration in Huntington's disease. J Cell Biol 194:209-227.
Kase BA, Northrup H, Morrison AC, Davidson CM, Goiffon AM, Fletcher JM, Ostermaier KK, Tyerman GH, Au KS (2012) Association of copper-zinc superoxide dismutase (SOD1) and manganese superoxide dismutase (SOD2) genes with nonsyndromic myelomeningocele. Birth Defects Res A Clin Mol Teratol 94:762-769.
Li R, Strykowski R, Meyer M, Mulcrone P, Krakora D, Suzuki M (2012) Male-specific differences in proliferation, neurogenesis, and sensitivity to oxidative stress in neural progenitor cells derived from a rat model of ALS. PLoS One 7:e48581.
Lim MA, Selak MA, Xiang Z, Krainc D, Neve RL, KraemerBC, Watts JL, Kalb RG (2012) Reduced activity of AMP-activated protein kinase protects against genetic models of motor neuron disease. J Neurosci 32:1123-1141.
Liu Z, Martin LJ (2006) The adult neural stem and progenitor cell niche is altered in amyotrophic lateral sclerosis mouse brain. J Comp Neurol 497:468-488.
Livak KJ, Schmittgen TD (2001) Analysis of relative gene expression data using real-time quantitative PCR and the 2(-Delta Delta C(T)) Method. Methods 25:402-408.
Lowry KS, Murray SS, McLean CA, Talman P, Mathers S, Lopes EC, Cheema SS (2001) A potential role for the p75 low-affinity neurotrophin receptor in spinal motor neuron degeneration in murine and human amyotrophic lateral sclerosis. Amyotroph Lateral Scler Other Motor Neuron Disord 2:127-134.
Luo Y, Xue H, Pardo AC, Mattson MP, Rao MS, MaragakisNJ (2007) Impaired SDF1/CXCR4 signaling in glial progenitors derived from SOD1(G93A) mice. J Neurosci Res 85:2422-2432.
Ma YC, Zhu R, Li JP (2012) Adenosine monophosphate-activated protein kinase and myofibrillar protein degradation. Zhongguo Zuzhi Gongcheng Yanjiu 16:341-344.
Martin E, Cazenave W, Cattaert D, Branchereau P (2013) Embryonic alteration of motoneuronal morphology induces hyperexcitability in the mouse model of amyotrophic lateral sclerosis. Neurobiol Dis 54:116-126.
Maruyama H, Morino H, Ito H, Izumi Y, Kato H, Watanabe Y, Kinoshita Y, Kamada M, Nodera H, Suzuki H (2010) Mutations of optineurin in amyotrophic lateral sclerosis. Nature 465:223-226.
Park HR, Kong KH, Yu BP, Mattson MP, Lee J (2012) Resveratrol inhibits the proliferation of neural progenitor cells and hippocampal neurogenesis. J Biol Chem 287:42588-42600.
Park M, Song KS, Kim HK, Park YJ, Kim HS, Bae MI, Lee J (2009) 2-Deoxy-d-glucose protects neural progenitor cells against oxidative stress through the activation of AMP-activated protein kinase. Neurosci Lett 449:201-206.
Rogers D, SchorNF (2010) The child is father to the man: developmental roles for proteins of importance for neurodegenerative disease. Ann Neurol 67:151-158.
Rosen DR (1993) Mutations in Cu/Zn superoxide dismutase gene are associated with familial amyotrophic lateral sclerosis. Nature 364:362.
Teng YD, Benn SC, Kalkanis SN, Shefner JM, Onario RC, Cheng B, Lachyankar MB, Marconi M, Li J, Yu D, Han I, Maragakis NJ, Llado J, Erkmen K, Redmond DE, Jr., Sidman RL, Przedborski S, Rothstein JD, Brown RH, Jr., Snyder EY (2012) Multimodal actions of neural stem cells in a mouse model of ALS: a meta-analysis. Sci Transl Med 4:165ra164.
van Zundert B, Peuscher MH, Hynynen M, Chen A, Neve RL, Brown RH, Jr., Constantine-Paton M, Bellingham MC (2008) Neonatal neuronal circuitry shows hyperexcitable disturbance in a mouse model of the adult-onset neurodegenerative disease amyotrophic lateral sclerosis. J Neurosci 28:10864-10874.
Wang XD, Morgan SC, Loeken MR (2011) Pax3 stimulates p53 ubiquitination and degradation independent of transcription. PLoS One 6:e29379.
Wu Y, Viana M, Thirumangalathu S, Loeken MR (2012) AMP-activated protein kinase mediates effects of oxidative stress on embryo gene expression in a mouse model of diabetic embryopathy. Diabetologia 55:245-254.
Ye X, Ma CC, Yao Y, Zang DW (2013) Synapsin expression of endogenous neural stem cell membrane in a mouse model of amyotrophic lateral sclerosis. Zhongguo Zuzhi Gongcheng Yanjiu 17:3527-3532.
YimMB, Kang JH, Yim HS, Kwak HS, Chock PB, Stadtman ER (1996) A gain-of-function of an amyotrophic lateral sclerosis-associated Cu, Zn-superoxide dismutase mutant: An enhancement of free radical formation due to a decrease in Km for hydrogen peroxide. Proc Natl Acad Sci U S A 93:5709-5714.
Zhu X, RainaAK, Perry G, Smith MA (2004) Alzheimer's disease: the two-hit hypothesis. Lancet Neurol 3:219-226.
Zhu X, Lee HG, Perry G, Smith MA (2007) Alzheimer disease, the two-hit hypothesis: an update. Biochim Biophys Acta 1772:494-502.

Copyedited by Cone L, Norman C, Wang J, Yang Y, Li CH, Song LP, Zhao M